2592 *Chem. Mater.* **2009,** *21,* 2592–2594
DOI:10.1021/cm900734c

CHEMISTRY OF
MATERIALS
Communication

Low-Dimensional Arylacetylenes for Solution-Processable Organic Field-Effect Transistors

Assunta Marrocchi,* Mirko Seri, Choongik Kim, Antonio Facchetti,* Aldo Taticchi,* and Tobin J. Marks*

Department of Chemistry, University of Perugia, Via Elce di Sotto 8, Perugia, Italy, and Department of Chemistry and the Materials Research Center, Northwestern University, 2145 Sheridan Road, Evanston, Illinois 60208

Received March 16, 2009
Revised Manuscript Received May 6, 2009

Organic semiconductors based on π-conjugated small molecules and polymers are widely studied as the charge transporting layer in organic field-effect transistors (OFETs). The development of solution-processable semiconductors is crucial from the OFET technological perspective to enable low-cost, large area, and mechanically flexible devices as well as to shed light on fundamental film growth processes from solution and charge transport characteristics. To this end, the most interesting semiconductor classes are soluble (hetero)acenes, oligothiophenes, and triphenylamines as well as polythiophenes and their copolymers.[1] With some of these semiconductors, field-effect mobilities (μ) up to ~2 cm^2 V^{-1} s^{-1} have been demonstrated using conventional oxide/polymeric dielectrics.[2] Recently, even greater FET performance has been obtained with polythiophenes in combination with polyelectrolyte dielectrics[3] and for solution-processed single-crystal OFETs.[4]

Despite these important achievements, it is desiderable to develop new solution-processable semiconductors to enhance our knowledge of molecular structure−FET property relationships. To this end, conjugated arylacetylenes may be a promising class of semiconductors suitable for OFET applications. It is known that their core functionalization with electron-donating or electron-withdrawing functional groups strongly modulates their physical and electronic properties.[5] Moreover, the π-conjugation length of these rod-like structures can be easily tuned by controlling the number of arylacetylene repeating units. For instance, a stable planar conformation of arylacetylenes is important for efficient molecular on−off conductance switching.[6] OFETs based on vacuum-deposited oligo(arylacetylene)s[7] exhibit μ values up to 0.3 cm^2 V^{-1} s^{-1} and $I_{\mathrm{on}}/I_{\mathrm{off}} \sim 10^5$, whereas known solution-processable arylacetylenes exhibit a maximum charge-carrier mobility of ~0.08 cm^2 V^{-1} s^{-1}.[8] Therefore, it is desirable to explore new structures to advance the state-of-the-art in performance. Furthermore, compared to the extended oligothiophene family, oligo(arylacetylene)s have been far less investigated.

In this communication we report the synthesis, characterization, and field-effect transistor response of soluble arylacetylene compounds **1** and **2**. In our design strategy, compound **1** (Figure 1) comprises an anthracene core linked to two repeating ethynylene−phenylene units at both 9,10-positions. This core is poorly polarizable and lacks substantial local dipoles because of the similarity of anthracene and phenyl electron donating/withdrawing capacities. However, despite the absence of local dipoles,[9] the use of the large anthracene as the core building block may favor substantial intermolecular overlap. Furthermore, it is more stable than larger acenes.[10] On the other hand, in compound **2** the apolar phenyl−ethyne−anthracene−ethyne−phenyl core of **1** is replaced with a donor−acceptor−donor (D-A-D, thiophene−benzothiadiazole−thiophene) motif.[11] This D-A-D unit enhances molecular rigidity and π-polarization,[12] affording low band gap semiconductors. Furthermore, mixing donor−acceptor units enhances dipole-induced intermolecular stacking.[11,13] This combination of a rod-like motif, large π-conjugation lengths extending along the molecular long axis, and substantial intermolecular overlap are important requirements for efficient charge transport.[1d,14] Finally, the flexible

---

(1) (a) Steckler, T. T.; Zhang, X.; Hwang, J.; Honeyager, R.; Ohira, S.; Zhang, X.-H.; Grant, A.; Ellinger, S.; Odom, S. A.; Sweat, A.; Tanner, D. B.; Rinzler, D.; Barlow, S.; Bredas, J.-L.; Kippelen, B.; Marder, S; Reynolds, J. R. *J. Am. Chem. Soc.* **2009**, *131*, 2824. (b) Videlot-Ackermann, C.; Brisset, H.; Zhang, J.; Ackermann, J.; Nenon, S.; Fages, S.; Marsal, P.; Tanisawa, T; Yoshimoto, N. *J. Phys. Chem. C* **2009**, *113*, 1567. (c) Allard, S.; Forster, M.; Souharce, B.; Thiem, H.; Sherf, U. *Angew. Chem., Int. Ed.* **2008**, *47*, 4070. (d) Facchetti, A. *Mater. Today* **2007**, *10*, 28.

(2) (a) Rincon Llorente, G.; Dufourg-Madec, M.-B.; Crouch, D. J.; Pritchard, R. G.; Ogier, S.; Yeates, S. G. *Chem. Commun.* **2009**, DOI: 10.1039/b901448a. (b) Park, S. K.; Mourey, D. A.; Subramanian, S.; Anthony, J. E.; Jackson, T. N. *Appl. Phys. Lett.* **2008**, *93*, 043301.

(3) Panzer, M. J.; Frisbie, C. D. *J. Am. Chem. Soc.* **2007**, *129*, 6599.

(4) (a) Reese, C.; Bao, Z. *Mater. Today* **2007**, *10*, 20. (b) Podzorov, V.; Menard, E.; Borissov, A.; Kiryukhin, V.; Rogers, J. A.; Gershenson, M. E. *Phys. Rev. Lett.* **2004**, *93*, 086602.

(5) (a) Li, C.; Li, Y. *Macromol. Chem. Phys.* **2008**, *209*, 1541. (b) Bunz, U. H. F. *Chem. Rev.* **2000**, *100*, 1605.

(6) Donhauser, Z. J.; Mantooth, B. A.; Kelly, K. F.; Bumm, L. A.; Monnel, J. D.; Stapleton, J. J.; Price, D. W.; Rawlett, A. M.; Allara, D. L.; Tour, J. M.; Weiss, P. J. *Science* **2001**, *292*, 2303.

(7) Roy, V. A. L.; Zhi, Y.-G.; Xu, Z.-X.; Yu, S.-C.; Chan, P. W. H.; Che, C.-M. *Adv. Mater.* **2005**, *17*, 1258–1261.

(8) Baek, N. S.; Hau, S. K.; Yip, H.-L.; Acton, O.; Chen, K.-S; Jen, A. K.-Y. *Chem. Mater.* **2008**, *20*, 5734.

(9) Anthony, J. E. *Chem. Rev.* **2006**, *106*, 5028.

(10) (a) Meng, H; Sun, F.; Goldfinger, A. B.; Jaycox, G. D.; Li, Z.; Marshall, J.; Blackman, G. S. *J. Am. Chem. Soc.* **2005**, *127*, 2406. (b) Ito, K.; Suzuki, T.; Sakamoto, Y.; Kubota, D.; Inoue, Y.; Sato, F.; Tokito, S. *Angew. Chem., Int. Ed.* **2003**, *42*, 1159.

(11) Sonar, P.; Singh, S. P.; Sudhakar, S.; Dodabalapur, A.; Sellinger, A. *Chem. Mater.* **2008**, *20*, 3184.

(12) (a) Mullekom, H.A.M. van; Venkemans, J. A. J. M.; Meijer, E. W. *Chem.—Eur. J.* **1998**, *4*, 1235. (b) Karikomi, M.; Kitamura, C.; Tanaka, S.; Yamashita, Y. *J. Am. Chem. Soc.* **1995**, *117*, 6791.

(13) Park, Y. S.; Kim, D.; Hoosung, L.; Moon, B. *Org. Lett.* **2006**, *8*, 4702.

(14) Schwab, P. F. H.; Levin, M. D.; Michl, J. *Chem. Rev.* **1999**, *99*(7), 1863.

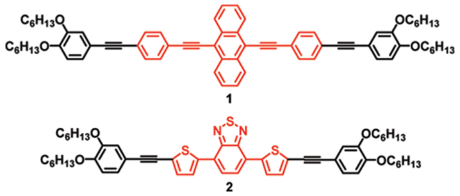

Figure 1. Chemical structure of compounds **1** and **2**.

hexyloxy chains at 3- and 4- positions of the terminal phenyl ring systems are introduced to solubilize both compounds in common organic solvents as well as to promote their self-organization in the solid state.[15] Indeed, hexyloxy chains at the 4-positions, that is, along the molecular main axis, may also lead to a better $\pi-\pi$ stacking, thus improving charge transport properties. Our results demonstrate solution-processed OFETs based on nonpolymeric arylacetylenes affording hole mobilities approaching 0.1 cm^2 V^{-1} s^{-1} in ambient conditions.

Compound **1** was synthesized according to our previously reported procedure,[16] while compound **2** was obtained in 90% yields by Pd/Cu catalyzed Sonogashira coupling bis(bromothienyl)-benzothiadiazole[17] with 3,4-(bishexyloxy)-ethynylbenzene.[18] These compounds were characterized via conventional spectroscopic and microanalytical techniques (see Supporting Information).

The redox properties of these systems were investigated by cyclic voltammetry (CV, see Figure S1 in Supporting Information), and the results are summarized in Table 1. Compound **1** exhibits the onset of oxidation at +0.64 V (vs Fc/Fc$^+$), with two irreversible events at +0.74 V and +1.10 V. A significant reduction wave is not observed. This result suggests that **1** may be intrinsically a better hole (p-type) charge transporter than an electron (n-type) semiconductor. Compound **2** exhibits one reversible oxidation wave with onset at +0.48 V and half-wave potential ($E^{1/2}$) of +0.53 V. Reduction of this material occurs whith an onset of −1.26 V and two reversible events ($E_1^{1/2} = -1.37$ V, $E_2^{1/2} = -1.64$ V) followed by an additional irreversible one at −2.07 V. Optical absorption data for compounds **1** and **2** in chloroform and as thin films are summarized in Table 1 (Figure S2, Supporting Information). The solid state spectra of both compounds are red-shifted relative to the solution spectra. This result suggests a better degree of molecular π-conjugation in the solid state and/or formation of J-aggregates. However, the introduction of a D-A-D moiety in **2** results in a substantial red-shift absorption and reduced bandgap as observed for other donor−acceptor structures.[19] Using optical absorption and cyclic voltammetry data, HOMO energy levels of −5.44 and −5.33 eV and the LUMO levels of −3.04 and −3.21 eV are estimated[20] for **1** and **2**, respectively. While the HOMO energies are suitable for OFET hole injection/transport, the LUMO energies of these systems are quite high for efficient electron transport. Finally, thermogravimetric analysis (TGA) was performed to evaluate the thermal properties of arylacetylenes **1** and **2**. The TGA plots (Figure S3, Supporting Information) indicate that both arylacetylenes are thermally stable, with onset decomposition temperatures of 276 °C for **1**[16] and 310 °C for **2**.

Table 1. Electrochemical and Optical Properties and MO Energies of Compounds 1[16] and 2

	E_{ox}[a] (V)	E_{red}[a] (V)	λ_{max}[b] [nm]	λ_{max} film [nm]	E_g[c] (eV)	E_{HOMO} (eV)	E_{LUMO} (eV)
1	0.64	−1.64	331, 464, 488	366, 438, 481, 514	2.40	−5.44	−3.04
2	0.48	−1.26	358, 504	357, 508, 563	2.12	−5.33	−3.21

[a] Determined vs Fc/Fc$^+$; onset values. [b] CHCl$_3$ solution. [c] Determined from the onset of the absorption in the thin film spectra.

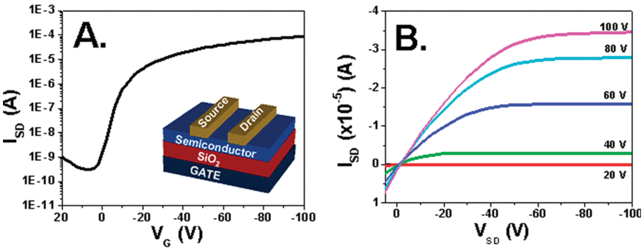

Figure 2. Transfer (A) and output (B) plots of semiconductor **1** on bare SiO$_2$. Device measured in vacuum.

Bottom-gate top-contact OFETs (Figure 2A, inset) were fabricated by spin-coating semiconductor solutions in CHCl$_3$ (5 mg/mL) on doped Si(gate)/SiO$_2$ (dielectric layer, 300 nm thick) substrates. These substrates were used without dielectric surface treatment (bare), treated with hexamethyldisylazane (HDMS), or treated with octadecyltrichlorosylane (OTS). Vacuum-deposited Au source and drain electrodes completed the FET structure. Device fabrication and characterization details are given in the Supporting Information. Representative transfer/output plots for compounds **1** and **2** are shown in Figures 2 and S4−7 (Supporting Information).

The negative gate and source-drain voltages demonstrate that both compounds are p-channel materials. This is consistent with previous reports on phenyleneacetylenes and the aforementioned HOMO energy values which are accessible for efficient hole injection from Au contacts. Table 2 summarizes FET response for all devices where the semiconductor film was annealed at 80 °C before Au deposition. Film thermal annealing from 40 to 80 °C generally improved device performance in terms of both mobility and I_{on}/I_{off}. However, higher annealing

---

(15) (a) Sung, A.; Ling, M.; Tang, M. L.; Bao, Z.; Locklin, J. *Chem. Mater*. **2007**, *19*, 2342. (b) Wurthner, F.; Schmidt, R. *Chem. Phys. Chem*. **2006**, *7*, 793. (c) Locklin, J.; Roberts, M. E.; Mannsfeld, S. C. B.; Bao, Z. *Polym. Rev*. **2006**, *46*, 79.

(16) Marrocchi, A.; Silvestri, F.; Seri, M.; Facchetti, A.; Taticchi, A.; Marks, T. J. *Chem. Commun*. **2009**, 1380.

(17) Kato, S.-I.; Matsumoto, T.; Ishi-i, T.; Thiemann, T.; Shigeiwa, M.; Gorohmaru, H.; Maeda, S.; Yamashita, Y.; Mataka, S. *Chem. Commun*. **2004**, 2342.

(18) Valentini, L.; Bagnis, D.; Marrocchi, A.; Seri, M.; Taticchi, A.; Kenny, J. M. *Chem. Mater*. **2008**, *20*, 32.

(19) (a) Kron, R.; Lenes, M.; Hummelen, J. C.; Blom, P. W. M.; De Boer, B. *Polym. Rev*. **2008**, *48*, 531. (b) Zhu, Z.; Waller, D.; Gaudiana, R.; Morana, M.; Mühlbacher, D.; Sharber, M.; Brabec, C. *Macromolecules* **2007**, *40*, 1981. (c) Blouin, N.; Michaud, A.; Leclerc, M. *Adv. Mater*. **2007**, *19*, 2295.

(20) Wu, C.-C.; Sturm, J. C.; Register, R. A.; Tian, J.; Dana, E. P.; Thompson, M. E. *IEEE Trans. Electron Devices* **1997**, *44*(8), 1269.

Table 2. Bottom-Gate Top-Contact OFET Characteristics of Compounds 1 and 2[a]

	surface treatment	μ^b (cm^2 V^{-1} s^{-1})		I_{on}/I_{off}		V_{ON} (V)		V_T (V)	
		vac	air	vac	air	vac	air	vac	air
1	bare	7×10^{-2}	7×10^{-2}	3×10^5	2×10^2	0	−22	−8	−22
	HMDS	5×10^{-2}	4×10^{-2}	8×10^5	6×10^6	−15	−17	−27	−30
	OTS[c]	3×10^{-2}	2×10^{-2}	4×10^5	2×10^6	−13	−51	−30	−55
2	bare	2×10^{-2}	2×10^{-2}	1×10^4	5×10^3	−3	−25	−7	−25
	HMDS	3×10^{-2}	2×10^{-2}	4×10^5	3×10^7	−8	−11	−20	−20
	OTS[c]	5×10^{-2}	4×10^{-2}	9×10^2	7×10^3	−12	−28	−20	−30

[a] SiO_2, 300 nm; annealing temperature (time), 80 °C (2 h); active layer, 30 nm; S/D electrode, 50 nm Au; *L*/*W*, 100 μm/5000 μm. [b] Maximum mobility values. [c] *L*/*W*: 100 μm/2000 μm.

temperatures (120 °C) have detrimental effects on the performance of both compounds. Semiconductors **1** and **2** exhibit hole mobilities up to ~0.07 cm^2 V^{-1} s^{-1} and ~0.05 cm^2 V^{-1} s^{-1}, respectively, and I_{on}/I_{off} approaching ~10^6 when measured in vacuum. Average mobilities are reported in Table S1 (Supporting Information) The electrical measurements performed in air reveal no substantial changes in charge carrier mobilities, whereas the I_{on}/I_{off} slightly decreases for some devices. Since this behavior is erratic, it may be the result of the unpatterned semiconductor film which may be unintentionally doped by oxygen. This process is sensitive to the film morphology, as seen for several oligo/polythiophenes.[21]

It is interesting to analyze how the FET performance changes by modifying the dielectric surface. Going from bare to HMDS- to OTS-treated Si/SiO_2 substrates, hence by increasing the dielectric surface hydrophobic character, the mobilities for **1** and **2** exhibit an opposite trend. This effect may be related to the different **1** and **2** charge distribution at the molecular level, which may modify the semiconductor film organization/self-assembly at the interface with the dielectric layer, depending on the dielectric surface energy. Given that both molecules are functionalized with apolar hydrocarbon chains, we speculate that the absence of substantial local dipoles in **1** reduces its core affinity for the hydrophilic/polar SiO_2 surface and enhances an ordered edge-on semiconductor morphology at the dielectric−semiconductor interface when the hydrophobicity increases. For the locally high polarity core of **2**, an opposite trend in molecular verus surface affinity is expected, with a better organized interface on apolar OTS versus hydrophilic bare substrates. However, as the AFM/XRD studies suggest (vide infra), these subtle interfacial effects do not alter the overall bulk film morphology and microstructure. Therefore, other effects such as dielectric surface chemistry and topology, affecting charge trap density, cannot be ruled out.

Tapping-mode atomic force microscopy (AFM, Supporting Information Figure S10) was employed to evaluate the arylacetylene thin film surface morphology and roughness. AFM analysis of **1**-derived films on both bare and OTS-treated Si/SiO_2 substrate reveal large crystal-like features protruding from the thin film surface (Figure S10A,B) and similar surface roughness of ~3.2−3.5 nm. On the other hand, films of compound **2** exhibit more homogeneous morphologies when spin-cast on bare (rms roughness = 2.05 nm) and then on OTS-treated (rms roughness = 6.05 nm) Si/SiO_2 substrates (Figure S10D,E respectively).

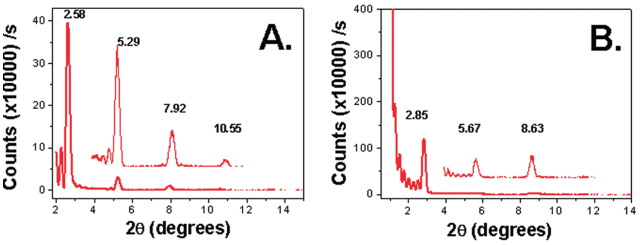

Figure 3. XRD scans for films of (A) semiconductor **1** and (B) semiconductor **2** spin-cast from chloroform onto bare Si/SiO_2 and annealed at 80 °C.

Thin-film X-ray diffraction (XRD, Figure 3, and Supporting Information Figure S8) $\theta-2\theta$ scans of arylacetylenes **1** and **2** were performed to investigate the degree of film crystallinity and the bulk molecular orientation with respect to the substrate surface. The XRD plots shown in Figure 3A and SI Figure S9B confirm the high crystallinity of **1** and **2** films resulting in optimum TFT performance (Table 2) which exhibit Bragg reflections up to the fourth and third order, respectively. Distinct primary reflections are observed at 2θ ~ 2.5° for **1** (*d*-spacings ~ 34 Å) and 2θ ~ 2.8° for compound **2** (*d*-spacings ~ 31 Å). Considering the semiempirical AM1-calculated molecular length of these systems (46.33 Å and 38.27 Å, respectively), these data are consistent with bulk film microstructures with an "edge-on" molecular orientation, consistent with the overall large FET mobilities. Clearly visible Laue oscillations demonstrate the uniform and smooth film morphologies. Similar morphologies are observed on HMDS substrates, although **1** films are somewhat less textured.

In conclusion, we have reported the synthesis and characterization of new arylacetylene-based molecular p-type semiconductors for FETs. Solution-processed OFETs based on these compounds exhibit high charge carrier mobility under ambient conditions. Studies are currently underway to further optimize molecular architectures and device characteristics.

Acknowledgment. We thank MIUR (Ministero dell'Istruzione, dell'Università e della Ricerca, Rome - Italy) and AFOSR (FA9550-08-1-0331) for financial support. We thank the NSF-MRSEC program through the Northwestern Materials Research Center (DMR-0520513) for providing characterization facilities.

Supporting Information Available: Synthetic procedure/spectroscopic data for **2**, device fabrication details, electrochemical/UV−vis/FET data, and XRD/AFM images (PDF). This material is available free of charge via the Internet at http://pubs.acs.org.

---

(21) (a) Meijer, E. J.; Detcheverry, C.; Baesjou, P. J.; van Veenendaal, E.; de Leew, D. M.; Klapwijk, T. M. *J. Appl. Phys.* **2003**, *93*, 4831. (b) Bao, Z.; Dodabalapur, A.; Lovinger, A. *J. Appl. Phys. Lett.* **1996**, *69*, 4108.